AMERICAN SOCIETY FOR MICROBIOLOGY | Infection and Immunity®

HOST RESPONSE AND INFLAMMATION

In *Staphylococcus aureus*, the Particulate State of the Cell Envelope Is Required for the Efficient Induction of Host Defense Responses

ByungHyun Kim,[a] TingTing Jiang,[a] Jun-Hyun Bae,[a] Hye Su Yun,[a] Seong Han Jang,[a] Jung Hyun Kim,[a] Jae Deog Kim,[a] Jin-Hoe Hur,[b] Kensuke Shibata,[c] Kenji Kurokawa,[d] Yunjin Jung,[a] Andreas Peschel,[e] Taeok Bae,[f] Bok Luel Lee[a]

[a]Host Defense Protein Laboratory, College of Pharmacy, Pusan National University, Busan, Republic of Korea
[b]UNIST-Olympus Biomed Imaging Center, UNIST, Ulsan, Republic of Korea
[c]Department of Microbiology and Immunology, Yamaguchi University, Graduate School of Medicine, Yamaguchi, Japan
[d]Faculty of Pharmaceutical Sciences, Nagasaki International University, Sasebo, Nagasaki, Japan
[e]Interfaculty Institute of Microbiology and Infection Medicine, Infection Biology, University of Tübingen, Tübingen, Germany
[f]Department of Microbiology and Immunology, Indiana University School of Medicine-Northwest, Gary, Indiana, USA

ABSTRACT Upon microbial infection, host immune cells recognize bacterial cell envelope components through cognate receptors. Although bacterial cell envelope components function as innate immune molecules, the role of the physical state of the bacterial cell envelope (i.e., particulate versus soluble) in host immune activation has not been clearly defined. Here, using two different forms of the staphylococcal cell envelope of *Staphylococcus aureus* RN4220 and USA300 LAC strains, we provide biochemical and immunological evidence that the particulate state is required for the effective activation of host innate immune responses. In a murine model of peritoneal infection, the particulate form of the staphylococcal cell envelope (PCE) induced the production of chemokine (C-X-C motif) ligand 1 (CXCL1) and CC chemokine ligand 2 (CCL2), the chemotactic cytokines for neutrophils and monocytes, respectively, resulting in a strong influx of the phagocytes into the peritoneal cavity. In contrast, compared with PCE, the soluble form of cell envelope (SCE), which was derived from PCE by treatment with cell wall-hydrolyzing enzymes, showed minimal activity. PCE also induced the secretion of calprotectin (myeloid-related protein 8/14 [MRP8/14] complex), a phagocyte-derived antimicrobial protein, into the peritoneal cavity at a much higher level than did SCE. The injected PCE particles were phagocytosed by the infiltrated neutrophils and monocytes and then delivered to mediastinal draining lymph nodes. More importantly, intraperitoneally (i.p.) injected PCE efficiently protected mice from *S. aureus* infection, which was abolished by the depletion of either monocytes/macrophages or neutrophils. This study demonstrated that the physical state of bacterial cells is a critical factor for efficient host immune activation and the protection of hosts from staphylococcal infections.

KEYWORDS *Staphylococcus aureus*, cell envelope, chemokines, host defense, innate immunity, phagocytes

Staphylococcus aureus is a Gram-positive human pathogen causing a wide range of diseases in humans, ranging from skin and soft tissue infections to many life-threatening diseases, such as pneumonia, endocarditis, and sepsis (1). In particular, invasive infections caused by methicillin-resistant *S. aureus* (MRSA) are often intractable to antibiotic therapy, leading to recurrent diseases or deaths. To solve these serious problems, we need to develop new vaccines and find novel preventive strategies (2, 3). The bacterial cell envelope contains many molecules recognized by host immune cells. Therefore, the identification of bacterium-derived cell envelope components able to

Citation Kim B, Jiang T, Bae J-H, Yun HS, Jang SH, Kim JH, Kim JD, Hur J-H, Shibata K, Kurokawa K, Jung Y, Peschel A, Bae T, Lee BL. 2019. In *Staphylococcus aureus*, the particulate state of the cell envelope is required for the efficient induction of host defense responses. Infect Immun 87:e00674-19. https://doi.org/10.1128/IAI.00674-19.

Editor Victor J. Torres, New York University School of Medicine

Address correspondence to Bok Luel Lee, brlee@pusan.ac.kr.

B.K. and T.J. contributed equally to this article.

Received 26 August 2019
Accepted 16 September 2019
Accepted manuscript posted online 23 September 2019
Published 18 November 2019

induce effective innate responses is a promising tool to develop preventive strategies against *S. aureus* infection.

Host immune systems are classified into innate and acquired immunities. Innate immunity is carried out by professional phagocytic cells, such as neutrophils, macrophages, and dendritic cells. The phagocytic cells recognize the components of the bacterial cell envelope through their receptor molecules (4). The recognition of cell envelope components by neutrophils, macrophages, and dendritic cells is essential for the first line of the host defense to eliminate invading pathogenic microbes. Several different families of receptors recognizing *S. aureus* cell envelope components have been reported. For example, the staphylococcal lipoproteins (5), wall-teichoic acid (WTA) (6, 7), lipoteichoic acid (LTA) (8), and peptidoglycan (PGN) (9) are recognized by Toll-like receptor 2 (TLR-2), mannose-binding lectin (MBL), immunoglobulin superfamily (CRIg), and NOD-like receptors (NLRs), respectively.

Purified staphylococcal cell envelopes are water-insoluble particles due to highly cross-linked PGN structures (10, 11). This insoluble cell envelope contains not only the cell wall surface proteins (12) but also other host cell-modulating molecules (9, 13), such as WTA and PGN. LTA and lipoproteins are also retained in the preparation of the cell envelope. Upon treatment with PGN-hydrolyzing enzymes (e.g., lysozyme, mutanolysin, and lysostaphin), this insoluble cell envelope converts to the water-soluble state (9, 10). Although the interactions between bacterial components and their receptors have been intensively studied for their roles in host immune activation, it is not clearly defined how the physical state of the bacterial components plays a role in host immune activation and protection.

Microsized particles and nanoparticles have been reported to exhibit adjuvant activity (14). One of the main functions of particulate adjuvants, such as alum, is to activate host innate immunity or to induce inflammatory responses around injection sites (15). These insoluble particulate molecules are easily engulfed by host phagocytes and are then able to activate innate immune cells, leading to the production of host-derived cytokines, chemokines, and other factors (16). Therefore, the determination of the recognition mechanism of the *S. aureus*-derived particulate or soluble cell envelope by host immune cells will be important for the understanding of host innate immune responses against *S. aureus* infection and vaccine development.

In this study, to investigate the role of the physical state of the staphylococcal cell envelope in host defense responses, we generated the particulate cell envelope (PCE) from *S. aureus* RN4220 and USA300 LAC strains by mechanical breakage and extensive washing. We also converted PCE into soluble cell envelope (SCE) by treating PCE with peptidoglycan-hydrolyzing enzymes, such as lysostaphin and lysozyme. Using the two different forms of staphylococcal cell envelope containing the same antigenic determinants and pathogen-associated molecular pattern (PAMP) molecules, in this study, we compared their innate immune activation and protective effect in a murine model of peritoneal infection.

RESULTS

Characterization of staphylococcal PCE and SCE. We prepared staphylococcal PCE from the *S. aureus* RN4220 wild-type strain (referred to as RN4220-PCE) based on our published method (17, 18) (Fig. 1A). Particle size analysis showed that the RN4220-PCE had a mean particle size of 1.085 μm (Fig. 1B). The RN4220-SCE was prepared by digesting the wild-type PCE (WT-PCE) with recombinant lysostaphin and lysozyme, as described previously (17) (Fig. 1C). SDS-PAGE analysis of the RN4220-SCE showed multiple protein bands (Fig. 1D), of which the 48-kDa and 35-kDa bands were identified as the cell wall proteins SpA (*S. aureus* protein A) and IsdA (iron-regulated surface determinant A), respectively (see Fig. S1 in the supplemental material). Trifluoroacetic acid (TFA) treatment of RN4220-PCE released various sizes of WTA ribitol phosphate moieties (17, 19), confirming the presence of WTA in the RN4220-PCE (Fig. 1E). In a dot blot analysis, the RN4220-SCE showed a strong LTA signal, which was greatly reduced in the SCE prepared from the mutant of *ltaS*, the gene encoding the LTA synthase

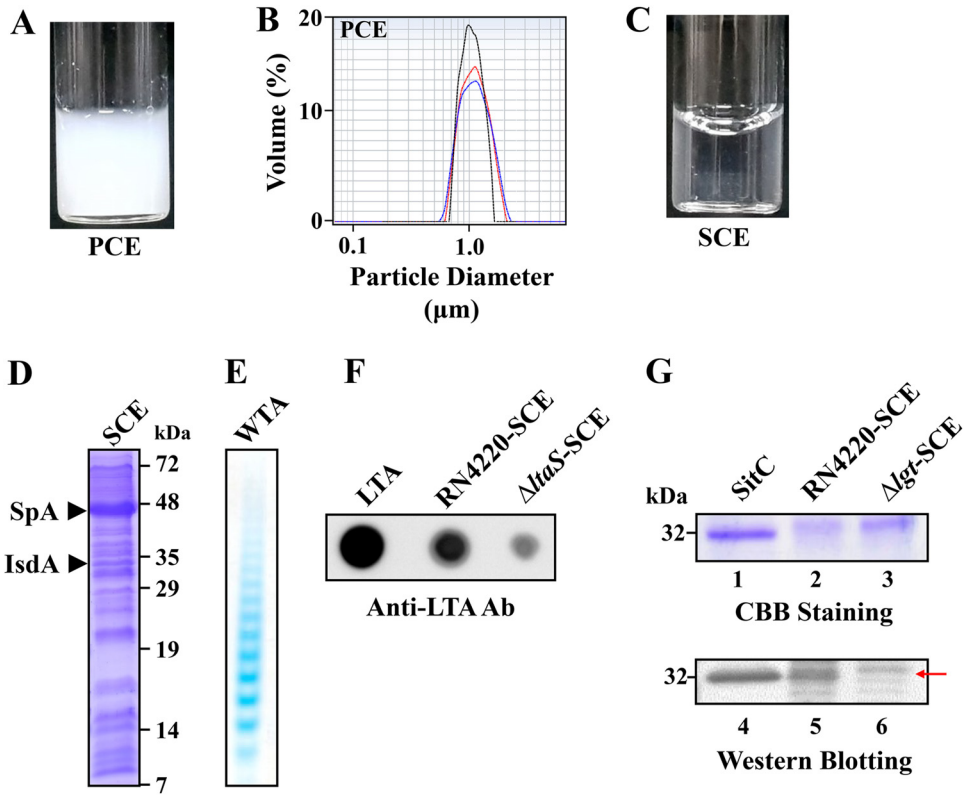

FIG 1 Biochemical characterization of WT-PCE and WT-SCE. (A and C) Photo images of WT-PCE (A) and WT-SCE (C). Lyophilized WT-PCE or WT-SCE (10 mg) was suspended 1 ml of PBS. (B) The particle size of WT-PCE was determined three times with a laser diffraction particle size analyzer (LS12 320 model; Beckman Coulter Co.). (D) The proteins (20 μg) of WT-SCE were analyzed by SDS-PAGE gels (15%) under reducing conditions. (E) The WTA ribitol phosphate molecules (10 μg) extracted from WT-PCE were separated by PAGE gels (27%) and visualized by alcian blue silver staining. (F) LTA analysis by dot blot immunoassay. SCEs (40 μg) prepared from the RN4220 wild type and Δ*ltaS* isogenic mutant were spotted on the PVDF membrane with LTA standard (5 μg; Sigma-Aldrich). Then, LTA was visualized by dot blot immunoassay with anti-LTA MAb (Invitrogen). (G) Lipoprotein analysis by Western blotting. After SDS-PAGE (upper row), the gel was immunoblotted (lower row), and then the presence of SitC lipoprotein was detected by anti-SitC polyclonal antibody, as described previously (43). The red arrow indicates the position of the SitC lipoprotein.

(Δ*ltaS*-SCE in Fig. 1F). Moreover, in a Western blot analysis, the lipoprotein SitC was detected in RN4220-SCE but not in SCE prepared from the mutant of *lgt*, the gene encoding lipoprotein diacylglycerol transferase (Fig. 1G). During the lipoprotein biosynthesis process, Lgt catalyzes the transfer of diacylglycerol to the sulfhydryl group of a cysteine residue in the signal peptide of lipoprotein precursors and is essential to anchor lipoproteins to the cell membrane (20). Finally, when the contents of D-Ala and *N*-acetylglucosamine (GlcNAc) in RN4220-PCE and RN4220-SCE were compared, no significant difference was observed (Fig. S2), indicating similar chemical compositions of the two samples. Taken together, these results demonstrate that the prepared WT-PCE and WT-SCE harbored all major staphylococcal cell envelope components (i.e., WTA, LTA, PGN, surface proteins, and lipoproteins) that can activate host innate immune responses.

PCE efficiently recruits major host phagocytes. To compare the innate immune activation capabilities of RN4220-PCE and RN4220-SCE, we injected RN4220-PCE or -SCE into mice via the intraperitoneal (i.p.) route and examined the recruitment of neutrophils and monocytes to the peritoneum. At 12 h after injection of five different doses of RN4220-PCE and -SCE, maximal numbers of neutrophils (35% of the total cell population) were recruited at amounts of ≥40 μg of RN4220-PCE injection (Fig. 2A). However, at the injection dose of 40 μg of RN4220-SCE, approximately five times fewer neutrophils (7% of the total cell population) were recruited. By injection of 160 μg of

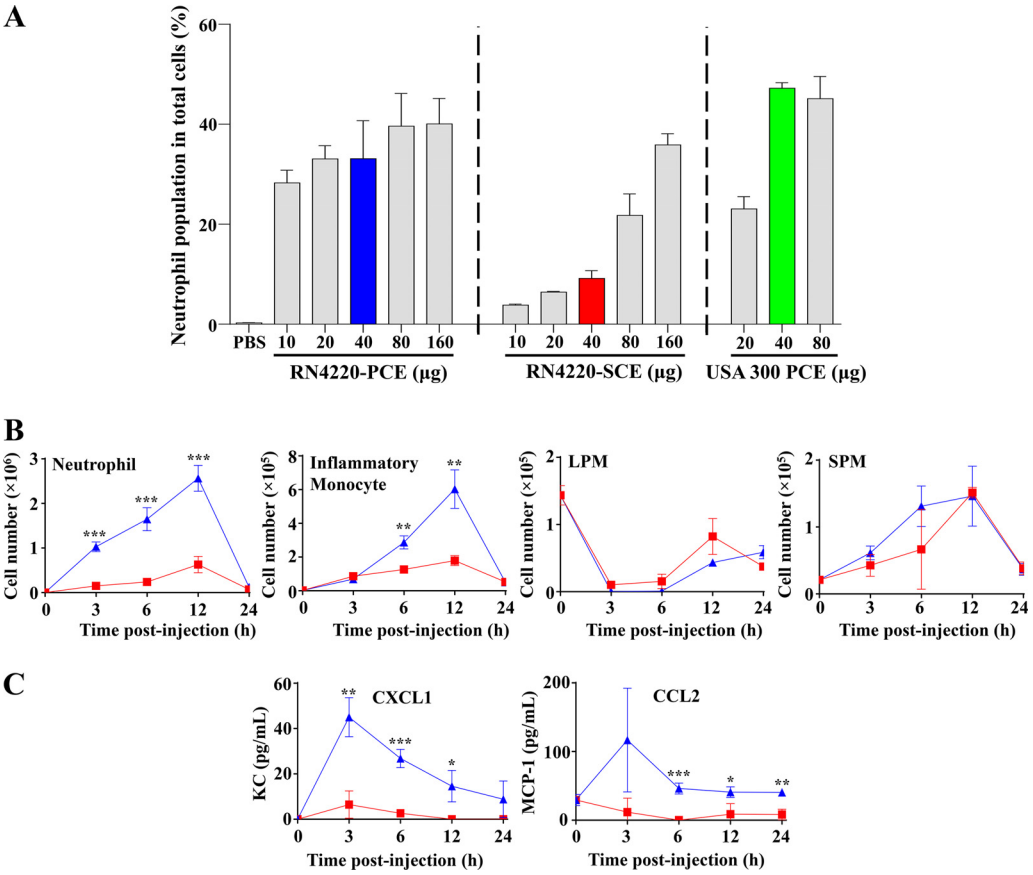

FIG 2 PCE recruits innate immune cells to the administration site. (A) The effect of staphylococcal envelope on the recruitment of neutrophils. Various amounts (10, 20, 40, 80, and 160 μg) of RN4220-PCE and -SCE and of USA300-PCE (20, 40, and 80 μg) were injected i.p. into mice. At 12 h postinjection, peritoneal lavage was carried out. Neutrophils were stained with fluorescein-conjugated antibodies (see Materials and Methods). Then, the numbers of the fluorescence-positive cells in 50,000 total cells were measured by FACS. (B) The effect of PCE and SCE on the recruitment of neutrophils, monocytes, and macrophages. Cells were detected by flow cytometry (Accuri C6 Plus; BD) with the following markers: neutrophils, Ly-6G$^-$ CD11b$^+$ F4/80$^+$ Ly-6C^{low}; inflammatory monocytes, Ly-6G$^-$ CD11b$^+$ F4/80$^+$ Ly-6C^{high}; large peritoneal macrophages (LPMs), F4/80$^+$ CD11b^{high} Ly6C$^-$; and small peritoneal macrophages (SPMs), F4/80^{low} CD11b$^+$ Ly6C$^-$. (C) Time-course analysis of chemokine production. Peritoneal fluid was collected as described above. Then, the chemokine levels (keratinocyte chemoattractant [KC] and monocyte chemoattractant protein [MCP]) were measured by the FACSArray bioanalyzer and FCAP Array software. Statistical analysis was performed using unpaired Student's *t* test (*, $P < 0.05$; **, $P < 0.01$; ***, $P < 0.0005$).

RN4220-SCE, almost the same numbers of neutrophils corresponding to 40 μg of RN4220-PCE were recruited, indicating that SCE is four to five times weaker than is PCE in recruiting neutrophils.

RN4220 is a laboratory strain containing multiple mutations (21). To examine whether the immune activation property of PCE is conserved in other clinical isolates of *S. aureus*, we repeated the experiment with PCE prepared from the USA300 LAC strain, a well-characterized clinical isolate (22). As shown in Fig. 2A, USA300-PCE recruited neutrophils as efficiently as RN4220-PCE, suggesting conservation of the neutrophil recruitment ability of PCE among different *S. aureus* strains. Here, for simplicity, we call RN4220-PCE and RN4220-SCE PCE and SCE, respectively.

Next, to test whether or not PCE treatment leads to the recruitment of different types of host immune cells, we analyzed the recruitment of four different host phagocytes, as follows (phenotype): neutrophils (Ly-6G$^+$ CD11b$^+$ F4/80$^-$ Ly-6C^{low}), inflammatory monocytes (Ly-6G$^-$ CD11b$^+$ F4/80$^+$ Ly-6C^{high}), large peritoneal macrophages (LPMs; F4/80$^+$ CD11b^{high} Ly6C$^-$), and small peritoneal macrophages (SPMs; F4/80^{low} CD11b$^+$ Ly6C$^-$) (23). The influx of neutrophils and monocytes was maximal at 12 h postinjection (Fig. 2B). Again, the number of recruited phagocytes by PCE was 4 to 5

times higher than that by SCE. Intriguingly, regardless of the antigens injected, the number of LPMs was significantly decreased by 6 h postinjection (LPM in Fig. 2B), whereas the number of SPMs slowly increased until 12 h postinjection (SPM in Fig. 2B). Nonetheless, there was no significant difference in the numbers of the recruited LPM and SPM between PCE- and SCE-injected mice, demonstrating that the distinct efficiency of cell recruitment between PCE and SCE applies mainly to neutrophils and monocytes.

The neutrophil chemokine (C-X-C motif) ligand 1 (CXCL1) and monocyte CC chemokine ligand 2 (CCL2) are known to attract neutrophils or monocytes (24). To understand the molecular basis of the higher recruitment of neutrophils and monocytes by PCE, we i.p. injected PCE and SCE into mice and, at various time points, measured the levels of CXCL1 and CCL2 in the murine peritoneum. Upon injection of PCE, the levels of both CXCL1 and CCL2 peaked at 3 h postinjection (Fig. 2C). Importantly, the levels of both chemokines were approximately 10 times higher in PCE-injected mice than those in SCE-injected mice, suggesting that PCE efficiently recruits neutrophils and monocytes to the injection site by inducing the secretion of the chemotactic chemokines CXCL1 and CCL2.

Only PCE is internalized by phagocytes and transferred into the mediastinal lymph node. Next, to examine whether the PCE and SCE are processed differently by innate immune cells, we labeled PCE and SCE with fluorescein 5-isothiocyanate (FITC). When the labeling efficiencies of PCE and SCE were examined by comparing the fluorescence intensities of equal amounts of the samples, no significant difference was observed (Fig. S3). The FITC-labeled PCE and SCE (40 μg each) were injected i.p. into mice. At 30 min, 1 h, and 2 h postinjection, peritoneal lavage was carried out. Then, three different peritoneal phagocytes were collected and examined by confocal microscopy (Fig. 3A). FITC signals were observed only inside the PCE-exposed neutrophils, LPMs and SPMs (Fig. 3A, left); no FITC signal was detected in the phagocytes exposed to FITC-SCE (Fig. 3A, right). These results demonstrated that the particulate state of PCE is critical for the engulfment by host phagocytes.

Of eight draining mouse lymph nodes (LNs), FITC signals were detected only in the mediastinal LN (mLN) of PCE-injected mice but not in SCE-injected mice (Fig. 3B). In mLN, the FITC-labeled PCE was found in neutrophils and inflammatory monocytes at 3 h and 6 h postinjection (Fig. 3C). Finally, when the numbers of neutrophils, monocytes, and dendritic cells in the mLN were measured after 6 h postinjection by flow cytometry, two to six times more phagocytes were detected in the PCE-injected mice than in SCE-injected mice (Fig. 3D). These results demonstrate that only PCE is taken up by phagocytes and transferred into the mLN.

PCE efficiently induces the release of calprotectin into peritoneal fluids. As a major cytoplasmic protein in neutrophils and monocytes, calprotectin is composed of myeloid-related protein 8 (MRP8) and 14 (MRP14) (25). The protein has antimicrobial activity and inhibits bacterial growth by depleting nutrient metals such as zinc and manganese (26). Also, this protein is an important component of neutrophil extracellular traps (NETs) (27). To examine whether the selective engulfment of PCE by neutrophils and monocytes affects the release of calprotectin, we injected PCE or SCE into mice via the i.p. route; then, at 12 h postinjection, peritoneal lavage was carried out. The peritoneal content was separated into peritoneal cells and peritoneal fluids (PFs). When equal amounts of the proteins of the peritoneal cell lysates (PCLs) and PFs were analyzed by 16% Tricine-6 M urea polyacrylamide gel electrophoresis, an 8-kDa protein band was enriched in the PCLs and PFs of the PCE-injected mice (Fig. 4A, asterisks). Edman sequencing confirmed that these 8-kDa bands were MRP8 (Fig. S4). When the PF fractions were further analyzed by Western blotting with antibodies raised against the commercially available recombinant MRP8 (rMRP8) and recombinant MRP14 (rMRP14) proteins, the 14-kDa MRP14 was detected only in the PF of PCE-injected mice (Fig. 4B, left), indicating that only PCE significantly induced the release of this protein. Intriguingly, with anti-rMRP8 antibody, no protein was detected, even in

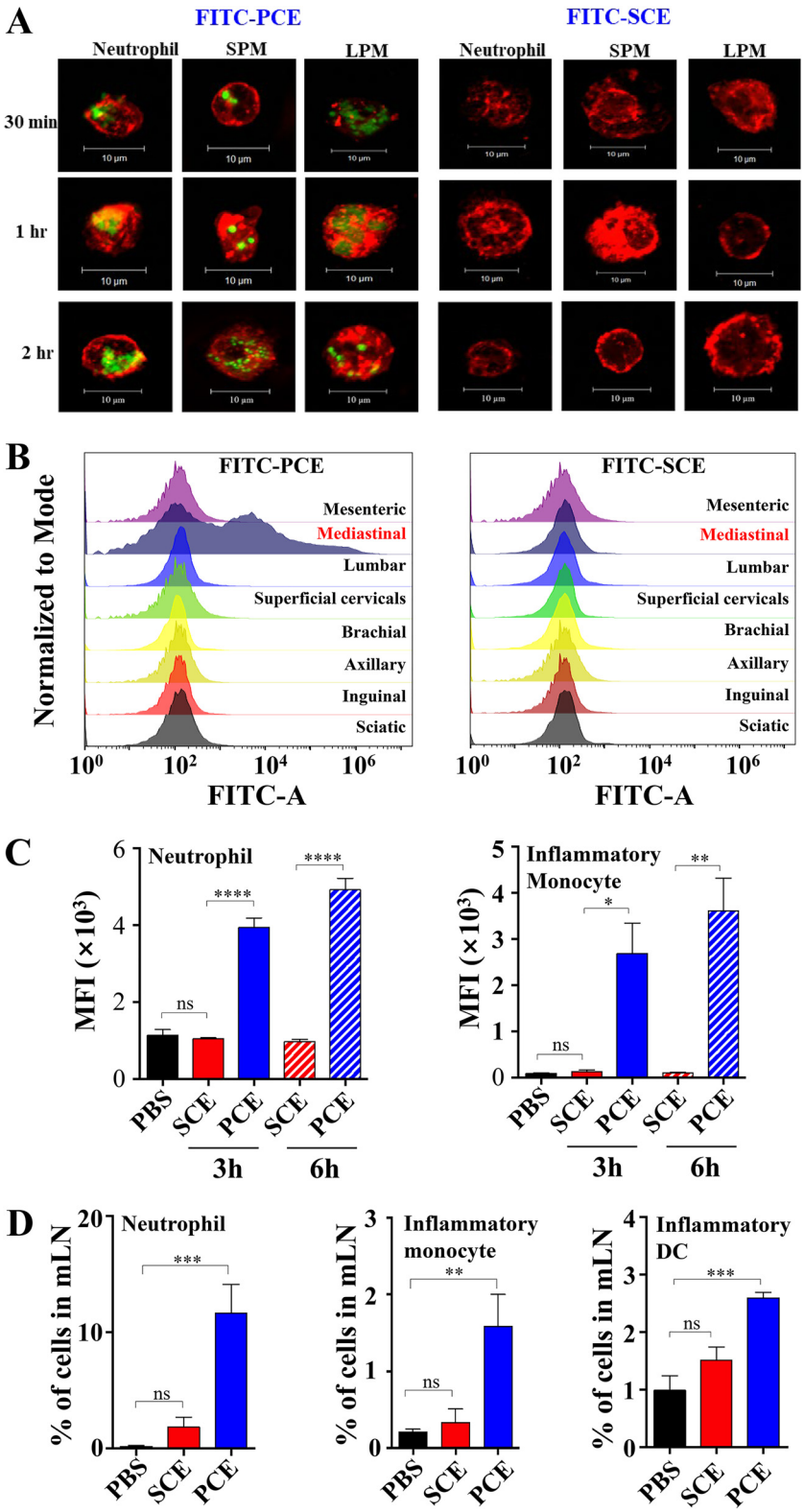

FIG 3 Recruited phagocytes engulf PCE and then migrate to mediastinal lymph node (mLN). (A) Mice were injected with FITC-PCE (40 μg) or FITC-SCE (40 μg). Then, 30 min, 1 h, and 2 h later, the peritoneal cells were collected. Neutrophils (CD11b$^+$ Ly6C$^+$ Ly6G^{high} F4/80$^-$), small peritoneal macrophages (SPMs; F4/80^{low} CD11b$^+$ Ly6C$^-$) and large peritoneal macrophages (LPMs; F4/80$^+$ CD11b^{high} Ly6C$^-$) were sorted by FACSAria high-speed sorter (BD Biosciences). The sorted cells were stained with 1 μM PKH26-GL red (Sigma-Aldrich) for 5 min and observed by confocal microscopy (LSM 700; Zeiss). (B) Six hours after i.p. injection of FITC-PCE (40 μg) or FITC-SCE (40 μg), eight different lymph nodes (LNs) were taken; then, LN

(Continued on next page)

the control lane (lane 5 of Fig. 4B), suggesting that, for an unknown reason, this protein is missing on the polyvinylidene fluoride (PVDF) membrane.

To understand the detection failure of MRP8 by Western blotting, we purified the native calprotectin (i.e., nMRP8/nMRP14 complex) from mouse neutrophils and then subjected the purified proteins to 16% Tricine–6 M urea polyacrylamide gel electrophoresis and Coomassie brilliant blue (CBB) staining. As expected, two bands of 14 kDa and 8 kDa were clearly observed ("Before" in Fig. 4C), indicating that native calprotectin was purified to homogeneity. When the proteins were electrotransferred onto the PVDF membrane, although no proteins remained in the PAGE gel, the 8-kDa MRP protein band was still missing in the PVDF membrane ("After" in Fig. 4C), suggesting that MRP8 passed through the PVDF membrane, probably due to its small size.

Since MRP8 passes through the PVDF membrane, we directly spotted rMRP8, rMRP14, and the purified calprotectin (nMRP8/nMRP14 complex) on the PVDF membrane and detected the proteins with anti-nMRP8 and anti-nMRP14 antibodies by dot blot immunoassay. As shown in Fig. 4D, not only rMRP14 but also rMRP8 was detected. More importantly, the purified calprotectin was also detected by both antibodies (lanes 7 and 14 in Fig. 4D).

With a dot blot immunoassay, we examined the PFs of mice injected with either PCE or SCE for MRP8 and MRP14 proteins. As shown in Fig. 4E, PFs from PCE-injected mice contained both MRP8 and MRP14 at much higher levels than those from the SCE-injected mice (lanes 6 versus 7 and 13 versus 14 in Fig. 4E). As expected, MRP14 was not detected in MRP14 knockout (KO) mice by PCE injection (Fig. 4F), confirming the specific secretion of calprotectin by PCE and specificity of the antibodies used in the assay.

Finally, we examined whether the release of calprotectin conferred antibacterial activity in the PF. The PFs were collected from the phosphate-buffered saline (PBS)-, SCE-, and PCE-injected mice at 12 h postinjection; then, the PFs were incubated with the *S. aureus* USA300 strain for 3 h. As shown in Fig. 4G, the PFs collected from PCE-injected mice suppressed bacterial growth approximately five times more than did the PFs from the SCE-injected mice (lanes 3 versus 4). The addition of $MnCl_2$ to the PCE-injected PF restored the bacterial growth (lanes 4 versus 5), demonstrating that the growth suppression was mainly due to the deprivation of manganese ions. Since manganese deprivation by calprotectin has been reported to reduce the activity of superoxide dismutase (SOD) of *S. aureus*, rendering the bacterium more susceptible to superoxide stress (28), we repeated the growth inhibition assay in the presence of Paraquat (1,1′-dimethyl-4,4′-bipyridinium dichloride), a superoxide-producing molecule (29). Although the addition of Paraquat reduced bacterial CFU in all samples, the reduction was most severe in the PF from PCE-injected mice; no bacteria were found (lane 9 in Fig. 4G), indicating a possible synergistic antibacterial effect of superoxide and $MnCl_2$ deprivation. Further addition of $MnCl_2$ significantly increased bacterial survival (lane 10). Taken together, these results demonstrate that PCE, but not SCE, not only efficiently recruits innate immune phagocytes but also activates the secretion of the antimicrobial protein calprotectin.

PCE, but not SCE, protects mice from staphylococcal infection. Since PCE particles induced much more efficient innate immune activation than did SCE, we further tested whether the activated host innate immunity would lead to better

FIG 3 Legend (Continued)
cells were prepared using a cell strainer. FITC intensity of the cell population was measured by flow cytometry. (C) After 3 h and 6 h injection of FITC-PCE or FITC-SCE, neutrophils and inflammatory monocytes of mLNs were gated, and then FITC signal-harboring neutrophils (left) and inflammatory monocytes (right) were counted by flow cytometry (Accuri C6 Plus; BD). (D) Mice were i.p. injected with PCE (40 μg) or SCE (40 μg). Six hours later, mLNs were collected, and the mLN total cells were incubated with antibody mixture for 10 min at 4°C. The numbers of neutrophils ($CD11b^+$ $Ly6G^+$ $F4/80^-$), inflammatory monocytes ($Ly6C^{high}$ $CD11b^+$ $F4/80^{low}$ $Ly6G^-$), and inflammatory DCs ($MHC\text{-}II^+$ $CD11c^+$ $CD11b^+$ $Ly\text{-}6C^+$) were counted among 50,000 cells by flow cytometry. Statistical analysis was performed using unpaired Student's *t* test (*, $P < 0.05$; **, $P < 0.01$; ***, $P < 0.001$; ****, $P < 0.0005$; ns, not significant).

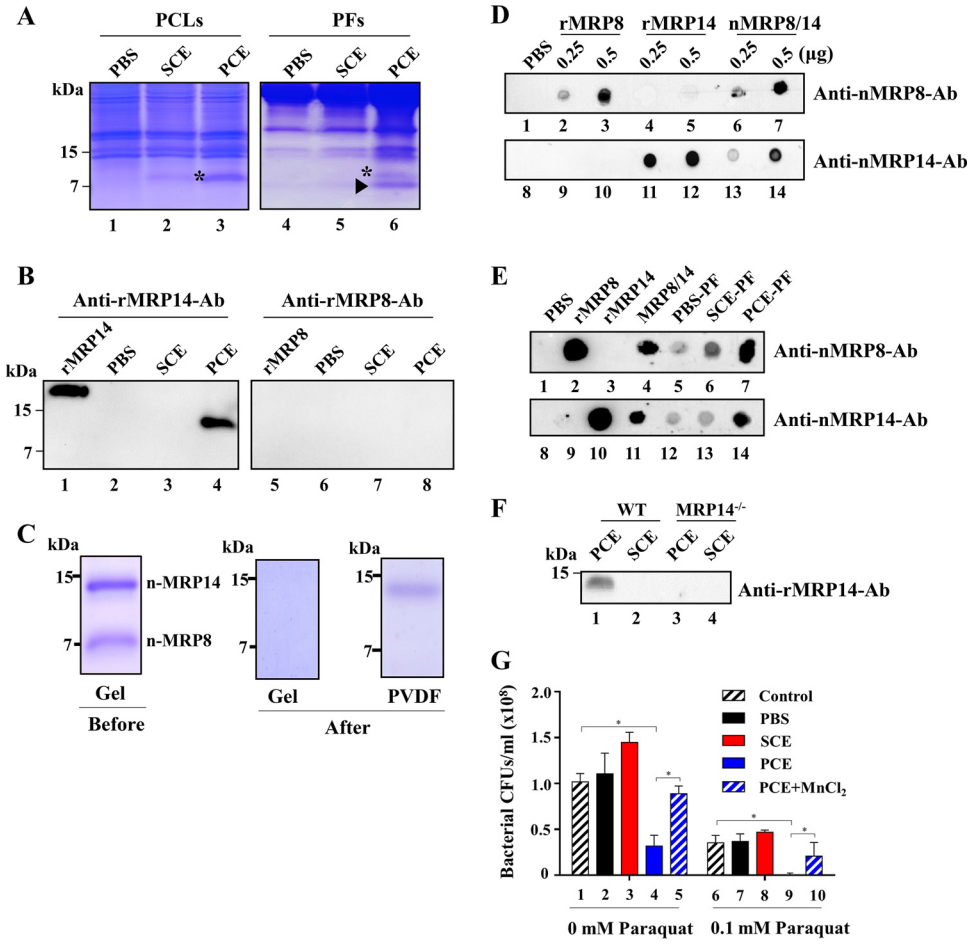

FIG 4 PCE induces the release of MRP8/14 (calprotectin) from recruited phagocytes. (A) Peritoneal cell lysates (PCLs; lanes 1 to 3) and peritoneal fluids (PFs; lanes 4 to 6) were obtained at 24 h postinjection of PBS, PCE, or SCE. Then, 20 μg of proteins was analyzed by 16% Tricine–6 M urea–0.1% SDS gel and Coomassie blue stain. Asterisks indicate enriched proteins in PCL and PF with 8-kDa molecular size. ▶, additional 7-kDa band in PF collected from PCE-injected mice. (B) Twenty microliters of PFs was further analyzed by Western blot analysis with anti-rMRP8 and anti-rMRP14 Abs (R&D Systems). (C) The same amounts (10 μg) of purified native MRP8 (nMRP8) and MRP14 (nMRP14) were separated on 16% Tricine–6 M urea–0.1% SDS gel and stained with Coomassie blue dye ("Before"). The proteins were subsequently electrotransferred onto PVDF membrane ("After"). (D) Determination of antibody specificity for rMRP8, rMRP14, or nMRP8/14. The proteins were dissolved in 50% ethanol, and the indicated amounts of proteins were spotted onto the PVDF membrane. Then, an immunoassay was carried out with anti-nMRP14 and anti-nMRP8 Abs. (E) Dot blot immunoassay to measure the release of MRP8 and MRP14 proteins into PFs. The rMRP8 (0.5 μg), rMRP14 (0.5 μg), purified nMRP8/14 (0.5 μg), and PFs from SCE- or PCE-injected mice (0.5 μg in 20 μl) were spotted on the PVDF membranes and subjected to the immunoassay with anti-nMRP8 and anti-nMRP14 antibodies. (F) PCE (40 μg) or SCE (40 μg) was injected i.p. into C57BL/6 WT and MRP14 deficient C57BL/6 S100A9$^{-/-}$ knockout mice. At 12 h postinjection, PFs were collected. The presence of MRP14 protein in each PF was examined by Western blot analysis with anti-rMRP14 Ab. (G) The antibacterial activity of PFs collected from SCE- or PCE-injected mice. PFs were mixed with USA300 cells in the absence (columns 1 to 5) and the presence (columns 6 to 10) of 1 mM Paraquat. To examine the effect of $MnCl_2$, $MnCl_2$ (10 μM) was added to PCE-PF. After 12 h of incubation, PFs were spread on the blood agar, and the CFU were measured.

protection against *S. aureus* infection. PCEs or SCEs were injected i.p. into mice; then, at 12 h postinjection, the mice were challenged with a lethal dose (5×10^8 CFU) of the *S. aureus* USA300 LAC strain via the i.p. route. As shown in Fig. 5A, PCE protected 90% of the mice ($n = 10$/group) from *S. aureus*-mediated death, whereas SCE protected only 20%, confirming that the PCE-mediated activation of innate immunity indeed more effectively protected the mice from *S. aureus* infection.

Upon PCE injection, neutrophils and monocytes were the predominant phagocytes recruited to the injection site (Fig. 2). To examine the roles of the recruited phagocytes in PCE-mediated protection, we reduced the numbers of neutrophils or monocytes/macrophages by administering either anti-Ly-6G monoclonal antibody (MAb) (30) or

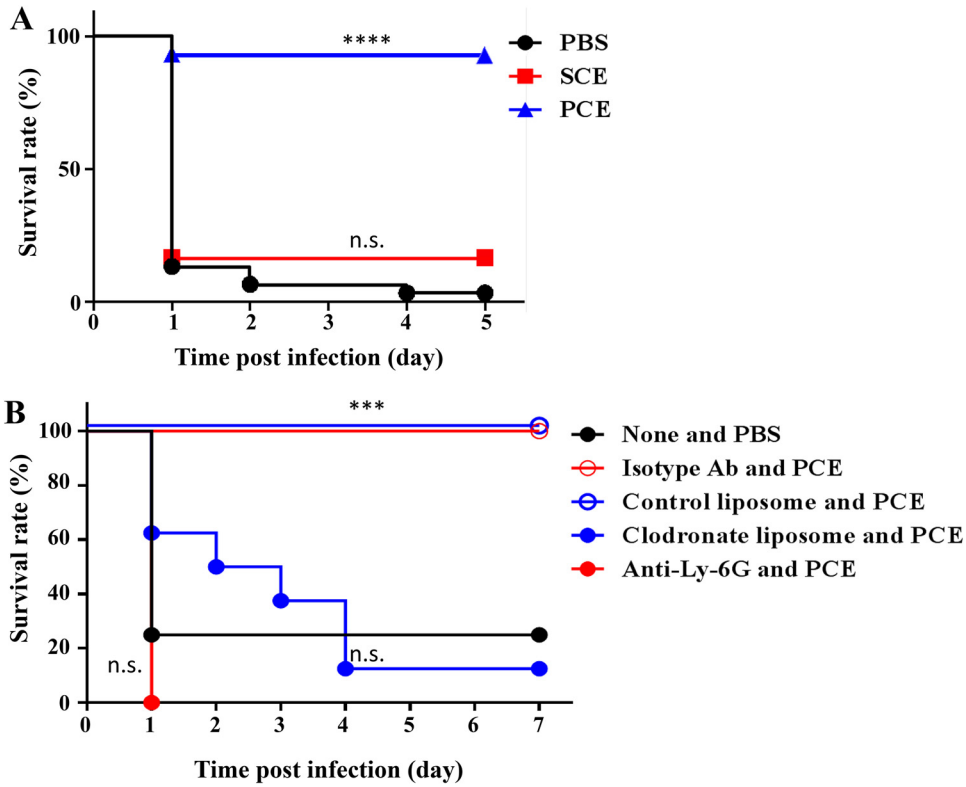

FIG 5 PCE-mediated innate immune response protects host from *S. aureus* infection. (A) The effect of PCE and SCE administration on the host survival. Phosphate-buffered saline (PBS; black circles), SCE (40 μg, red squares), and PCE (40 μg, blue triangles) were injected i.p. into 10 mice. At 12 h postinjection, USA300 cells were administered via i.p. injection, and the infected mice were watched for 5 days. (B) The role of neutrophils or monocytes/macrophages in the PCE-mediated protection against staphylococcal infection. Prior to PCE injection, the phagocytes were reduced by injecting anti-Ly-6G MAb (neutrophils) or clodronate liposome (monocytes/macrophages). Isotype-matched control antibody (i.e., rat IgG2a) and empty liposome were used as controls. After 12 h of PCE injection, the mice (n = 7 to 8) were challenged with i.p. injection of USA300 LAC cells (5×10^8 CFU/mouse) and observed for 7 days. Statistical significance of the murine survival between the PBS control condition (black circle) and the other test conditions was measured by log rank test. ***, $P < 0.005$; ****, $P < 0.0001$; n.s., not significant.

clodronate liposome (31, 32) via the tail vein. At 24 h postadministration, PCE was injected i.p. into the mice. Then, at 12 h postinjection, after confirming the reduced numbers of neutrophils or monocytes and macrophages (LPMs and SPMs) by flow cytometry (Fig. S5), the mice were challenged with a lethal dose of USA300 cells (5×10^8 CFU) via i.p. injection. As shown in Fig. 5B, all neutrophil-depleted mice (n = 8/8) died within 1 day, while, upon depletion of monocytes and macrophages, only one mouse (n = 1/8) survived by day 7. In contrast, all control mice (8 for isotype antibody [Ab] and 7 for control liposome) survived until day 7, demonstrating that both neutrophils and monocytes/macrophages play critical roles in the PCE-mediated protection against *S. aureus* infection.

DISCUSSION

Many bacterial cell envelope components function as innate immune molecules for host immunity (33). However, how the physical states of the bacterial cell envelope, particulate versus soluble, affect their immune activation efficiency is not studied. Here, we provide biochemical and immunological evidence that the particulate state of the staphylococcal cell envelope is required for efficient innate immune activation. Also, we showed that this innate immune activation and protection involve both neutrophils and monocytes/macrophages. In a recent work, the Underhill group reported that particulate fungal β-glucans of *Saccharomyces cerevisiae* cell wall activate the dectin-1 receptor via the formation of phagocytic synapse and triggering of the downstream

signaling events, resulting in the generation of reactive oxygen species (ROS) and the induction of antimicrobial activity (34). Like live fungi, the β-glucan particles caused the clustering of dectin-1 molecules and the formation of phagocytic cups. However, as with our observation with staphylococcal SCE, the soluble β-glycans failed to do so. These observations indicate that, for efficient innate immune defense against both bacteria and fungi, the particulate state of the invading pathogen is essential.

Despite the same antigenic composition, why is PCE much more efficient in innate immune activation than SCE? Although the exact molecular mechanisms are not yet clear, the higher local antigen density and the colocalization of multiple immune activators of the PCE likely contribute to the efficient receptor binding and subsequent innate immune activation. On the contrary, the injected SCE will disperse easily and be present at a much lower local concentration, which in turn is expected to lead to inefficient immune activation. Also, the particulate state itself seems to play a positive role in immune activation. For example, polystyrene particles measuring 430 nm to 1 μm efficiently activate dendritic cells to produce interleukin-1 beta (IL-1β) (35). The optimal size of silica for the engulfment by macrophages is approximately 1 μm (36). Therefore, the facile phagocytosis of PCE (Fig. 3) is also likely to contribute to the efficient antigen processing and innate immune activation, leading to the induction of subsequent antimicrobial responses, such as ROS production and calprotectin secretion.

Until this study, three molecules, uric acid (15), host DNA, (37) and lipid derivatives (38), were reported to be released from host cells upon injection of particulate adjuvants. Here, we provide the first biochemical evidence that staphylococcal PCE can also release calprotectin from host phagocytes (Fig. 4). The antimicrobial activity of calprotectin is expected to contribute to the faster elimination of *S. aureus* cells in the PCE-injected mice (Fig. 5A). If calprotectin was released by PCE, it is possible that other intracellular molecules, including DNA, can also be released. Since both DNA and calprotectin are important components of NETs (27), it is plausible that PCE also induced NET formation, which in turn further contributes to the elimination of bacterial cells. It remains to be determined how PCE induces the release of calprotectin from the phagocytes.

In this study, the injected i.p. PCE specifically migrated to the mediastinal LNs (Fig. 3B). Similar results were also reported previously with live *Listeria monocytogenes* or Indian ink particles (39). Upon i.p. injection, the live *L. monocytogenes* and Indian ink particles were phagocytosed by intraperitoneal macrophages and neutrophils and transported into the mLNs before they were spread to other body parts. The host phagocytes containing PCE or live bacterial cells probably migrate to mLNs via the afferent lymphatic vessels, giving rise to inflammatory responses. Therefore, it is likely that during intraperitoneal infections, the mediastinal LNs serve as a focal point from which the infectious agents will spread to adjoining organs, such as the liver, spleen, and kidneys, via the phagocytes.

Compared with peritoneal cell lysates (PCLs), peritoneal fluids (PFs) generated a unique 7-kDa band (▶ in Fig. 4A). Despite multiple trials to purify the protein or to analyze it with liquid chromatography-tandem mass spectrometry (LC-MS/MS), we failed to identify the nature of this band. Intriguingly, the 7-kDa band pattern is similar to that of the modified MRP8 band (40). Neutrophil-derived MRP8 and MRP14 are known to be readily *S*-nitrosylated at conserved cysteine residues by nitric oxide (NO) donors, such as *S*-nitroso-*N*-acetyl-penicillamine, *in vitro* (40). Although we cannot rule out the possibility that the 7-kDa protein is not MRP8, it is also possible that the unique 7-kDa band is the modified MRP8 protein. If that is the case, the absence of the 7-kDa band in peritoneal cell lysates suggests that the modification of the protein occurs during or after the release of the proteins. If so, it is of interest to determine what types of modifications occur to the proteins and whether the modifications affect the antimicrobial function of the proteins.

Upon recognition of bacterial cell wall components by receptors, the production of proinflammatory mediators, such as cytokines and chemokines, leads to infiltration of

neutrophils and macrophages, which are directly involved in the clearance of the pathogens (24). Also, the innate immune cells have the potential to elicit effective adaptive immunity, including helper T cell-mediated antibody production, and confer relatively long-term protective immunity (4). In the present study, we observed a release of calprotectin into the peritoneal fluid as a specific host defense molecule and migration of PCE-engulfed phagocytic cells into the mLNs upon injection. It will be interesting to see how PCE and SCE elicit different effects on acquired immunity in comparison to a well-known particulate adjuvant, such as alum.

Our findings in this study support the importance of the particulate state of the cell envelope in augmenting the host immune responses by the recruitment of host phagocytes. These phagocytes are capable of producing nonspecific antimicrobial molecules, such as calprotectin and ROS, and effectively eliminate invading *S. aureus* (39). However, unlike PCE, the live bacterium is capable of producing multiple toxins targeting those host phagocytes (40). For example, gamma-hemolysin AB and CB (HlgAB and HlgCB), the leucocidin AB and ED (LukAB and LukED), and Panton-Valentine leucocidin (PVL) can kill neutrophils, monocytes, and macrophages (41), rendering the host susceptible to *S. aureus* infection. Therefore, to develop a novel antitherapeutic agent against *S. aureus* infection, not only the bacterial antigens activating host immune responses but also the anti-toxin antibodies or toxin-neutralizing components should be considered.

MATERIALS AND METHODS

Ethics statement. Age- and sex-matched wild-type C57BL/6 mice, purchased from Orient Bio (Charles River Breeding Laboratories Korea), were kept in microisolator cages in a pathogen-free animal facility. The experiments were performed according to the institutional guidelines and approval (PNU-2017-1503) of the Pusan National University Institutional Animal Care and Use Committee (PNU-IACUC). Animal experiments using calprotectin-deficient (C57BL/6 S100A9$^{-/-}$) mice were performed at the Indiana University School of Medicine-Northwest (IUSM-NW), according to the protocol (NW-43) approved by the Institutional Animal Care and Use Committee of IUSM-NW. The calprotectin-deficient mice were acquired from the Vanderbilt University School of Medicine under permission from the University of Muenster. Every effort was made to minimize the suffering of the animals.

Bacteria. For the preparation of staphylococcal PCE and SCE samples, we used the *S. aureus* RN4220 wild-type strain (41), the LTA-deficient RN4220 Δ*ltaS* mutant strain (42), and the lipoprotein-deficient RN4220 Δ*lgt* mutant strain (43). The USA300 strain (44) was used for infection experiments.

Proteins. *S. aureus* SitC protein was purified as described previously (43). Native MRP8 (nMRP8) and native MRP14 (nMRP14) proteins were purified as described previously (45). Briefly, 1 ml of 9% casein solution (9 g of casein [Merck] dissolved in 100 ml of PBS [Lonza] containing 0.9 mM $CaCl_2$ and 0.6 mM $MgCl_2$ [pH 7.2]) was i.p. injected into mice (BALB/c, 9 weeks old, male, five mice/group). At 12 h postinjection, peritoneal fluid was collected with the harvest solution (PBS containing 0.05 mM EDTA), and then peritoneal exudate cells (PECs) were obtained by centrifugation at 300 × *g* and 4°C for 10 min. Using PECs, the neutrophils were separated using MACS cell separation columns (Miltenyi Biotec) and a neutrophil isolation kit (Miltenyi Biotec), following the manufacturer's recommended protocols. The collected neutrophils (5×10^7 cells from five mice) were added to 20 ml of cell lysis solution (25 mM Tris-HCl [pH 8.0], 1 mM EDTA, 1 mM EGTA, 1 mM dithiothreitol [DTT]). After suspension, ammonium sulfate powder (14.33 g) was added to 100% (wt/vol) final concentration. After 1 h, the mixture was centrifuged at 20,400 × *g* and 4°C for 30 min. After collection of the supernatant, 100% trichloroacetic acid (TCA) solution was added to 10% and incubated at 4°C for 60 min. After centrifugation at 20,400 × *g* and 4°C for 30 min, the obtained pellet was neutralized to pH 7.0 with 1 M KOH. The purity of the obtained pellet was examined by 16% Tricine–6 M urea–0.1% SDS gel or by a 15% SDS-PAGE gel under reducing conditions.

Preparation of PCE and SCE. PCEs and SCEs were prepared according to our published methods (17, 46), with some modification. Briefly, cultured *S. aureus* RN4220 cells were treated with 70% chilled ethanol for 1 h at 4°C. Subsequently, the killed bacteria were collected by centrifugation at 3,000 × *g* and 4°C for 10 min and washed three times with 20 ml of double-distilled water (DDW). The collected bacterial cells were lyophilized. Two hundred milligrams of lyophilized ethanol-killed bacteria was mixed with 12 g glass beads (diameter distributions between 0.10 and 0.11 mm; Sartorius AG, Inc.) in 20 ml of buffer A (20 mM citrate [pH 4.7], 1 M NaCl) and then disrupted with grinding homogenizer (Retsch, MM400 type). The glass beads were removed by centrifugation at 1,400 × *g* and 4°C for 10 min, and the cell envelope fraction was collected. The collected cell envelope was centrifuged again at 20,400 × *g* and 4°C for 10 min. After discarding the supernatant, the pellet was washed twice with 10 ml of buffer A. The pellet was suspended in 10 ml of buffer A and mixed with 10 ml of buffer A containing 1% SDS. The mixture was incubated at 60°C for 30 min and centrifuged at 20,400 × *g* and 20°C for 5 min. The remaining SDS was completely washed out from the pellet with DDW, and the pellet was finally suspended in DDW. The insoluble cell envelope suspension was frozen at −80°C and subsequently lyophilized. The obtained insoluble particulate cell envelope was referred to as PCE. Twenty milligrams

of lyophilized PCE was suspended with 1 ml of 25 mM phosphate buffer (pH 8.0), mixed with 80 μg of recombinant lysostaphin (LSPN; Ambi), and incubated at 37°C for 1 h. Afterwards, 4 μg of recombinant lysozyme (Lysobac; lnV_{iTRIA}) was added, and the sample was again incubated at 37°C for 1 h. The enzymes were inactivated at 60°C for 10 min and centrifuged at 216,000 $\times$ *g* and 4°C for 30 min. The supernatant was frozen at −80°C and lyophilized. The residue was referred to as SCE.

Quantification of D-Ala and GlcNAc in PCE and SCE. The amounts of D-Ala and of GlcNAc in PCE and SCE were measured as described previously (17, 46–49). To measure the amounts of D-Ala, three different batches (30 μg each) of PCE and SCE were incubated in 0.1 M NaOH at 37°C for 2 h and separated by thin-layer chromatography on silica gel 60 (Merck, Darmstadt, Germany) in a solvent consisting of *n*-propanol:pyridine:acetic acid:water (18:10:5:16). Then, the plate was treated with ninhydrin reagent to visualize amino groups of D-Ala residue, and the D-Ala amounts on the plate were quantified by a scanner (GDS200; Korea Lab Tech). The GlcNAc amounts in SCE and PCE were quantified as described previously (50). Briefly, three different batches (200 μg each) of SCE and PCE were hydrolyzed in 6 N HCl at 100°C for 3 h *in vacuo*, which is necessary to avoid the degradation of GlcNAc residues in the oxygen. Then, GlcNAc was quantified with the Morgan-Elson reagent.

Measurements of particle size. The mean and median particle sizes of PCE and SCE in PBS were determined by a laser diffraction particle size analyzer (LS12 320 model; Beckman Coulter Co.).

WTA preparation from WT-PCE. WTA was prepared according to our published method (17), with some modifications. Briefly, to release WTA, PCE (200 mg) was suspended in 10 ml of 12.5% TFA and incubated at 37°C for 12 h. The digested materials were centrifuged, and the WTA in the supernatant was precipitated with cold acetone. The ribitol phosphate moieties of the released WTA were confirmed by a 27% PAGE gel and alcian blue silver staining (19).

Analyses of chemokines and cytokines. One hundred micrograms of PCE and SCE in 100 μl of PBS was injected i.p. into the mice, and then the peritoneal lavage was carried out at 0, 1.5, 3, 6, 12, and 24 h postinjection with 5 ml of Hanks balanced salt solution (HBSS; Gibco) containing 0.5% bovine serum albumin (BSA) and 2 mM EDTA. The collected fluid was centrifuged at 4°C and 300 $\times$ *g* for 5 min. The supernatants were transferred to a 500-μl tube and kept at −80°C until use. Chemokine and cytokine levels were quantified with cytometric bead array mouse flex sets (BD Biosciences) and analyzed with FACSArray bioanalyzer and FCAP Array software.

Immunodot blotting. To confirm the presence of LTA in the SCEs or the detection of calprotectin in peritoneal cell lysates (PCLs) and peritoneal fluids (PFs), the immunodot blotting was carried out as described previously (51). Briefly, after activation of a PVDF membrane with methanol, samples were mixed with ethanol (final 50% concentration), spotted on the membrane, and dried. The membrane was blocked by soaking in 5% skim milk in 20 mM TBST (Tris-buffered saline [pH 7.4] containing 0.1% Tween 20) at room temperature (RT) for 1 h and then incubated with primary antibodies (1/500 dilution of anti-nMRP8 Ab and 1/1,000 dilution of anti-nMRP14 Ab) dissolved in skim milk-TBST at room temperature for 1 h. The membrane was washed three times with TBST for 10 min and incubated with secondary antibody conjugated with horseradish peroxidase (HRP; 1/5,000; Santa Cruz) at room temperature for 30 min. The membrane was washed three times with TBST for 10 min, incubated with enhanced chemiluminescence (ECL) reagent for 1 min, and then imaged with the Bio-Rad ChemiDoc system.

Flow cytometry. The following antibodies were purchased from either BD Biosciences or eBioscience: Ly-6G-APC, F4/80-PE, CD11b-FITC, and Ly-6C-PerCP (APC, allophycocyanin; PE, phycoerythrin; PerCP, peridinin chlorophyll protein). Typically, 200,000 cells were stained with specific MAbs after blockage of nonspecific binding by FcR blocking reagent (Miltenyi Biotec). Stained cells were analyzed on an Accuri C6 Plus flow cytometer (BD), and 10,000 to 20,000 events were collected for each analysis. Flow data were analyzed using the FlowJo software (Tree Star, Inc.).

Labeling of antigen with FITC. FITC labeling of PCEs or SCEs was performed using a method described by Tino and Wright (52). Briefly, PCE or SCE (10 mg) was suspended in 0.1 M sodium carbonate buffer (pH 8.5). Stock solution (1 mM) of fluorescein isothiocyanate (FITC; Sigma-Aldrich) was prepared with anhydrous dimethyl sulfoxide. One hundred microliters of FITC stock solution was added to PCE and SCE to a final concentration of 0.02 mM and then incubated at RT for 1 h. FITC-labeled PCE was washed out with DDW to remove unbound FITC. FITC-labeled SCE was separated from unbound FITC with Sephadex25 desalting column (GE Healthcare) connected to a high-performance liquid chromatography (HPLC) system (Gilson). Both samples were lyophilized and stored at −80°C until use.

To compare the FITC labeling efficiency, 1 mg of each of the lyophilized FITC-SCE and FITC-PCE was suspended in 1 ml PBS. Then, 40 μl of the samples was transferred into the wells of a black-colored 96-well plate (SPL Life Sciences), and fluorescence was measured using a multimode microplate reader (TriStar LB 941; excitation, 460 nm; emission, 510 nm, Berthold Technologies GmbH & Co.). This measurement was repeated two more times.

Phagocytosis analyses of FITC-labeled PCE and SCE. The phagocytosis assay was carried out by a method described by Geertsma et al. (53). Briefly, 40 μg of FITC-labeled PCE or SCE was injected i.p. into mice (five per group). At 30 min, 1 h, and 2 h postinjection, peritoneal cells were collected in RPMI medium containing 10% serum at 4°C and used immediately for sorting in the flow cytometer and cell sorter (FACSAria III; BD Biosciences). Three different types of phagocytes (i.e., neutrophils, small peritoneal macrophages [SPMs], and large peritoneal macrophages [LPMs]) were sorted. Cells (2×10^4) were mounted on a glass slide and incubated with 500 μl of 4% paraformaldehyde at room temperature for 10 min. The attached cells were stained with 2 μM PKH26-GL red (a fluorescent lipid-intercalating dye; Sigma-Aldrich) at 37°C for 5 min. To quench the fluorescence of the cell surface, cells were incubated with 300 μl of 0.4% trypan blue solution (Sigma-Aldrich) for 5 min. The cells were washed three times with

1 ml of PBS. After dropping 5 μl of fluorescent mounting solution (catalog no. S3023; Dako) on the glass slides, cells were examined with confocal microscopy (LSM 700; Zeiss).

Migration analysis of FITC-PCE and -SCE into LNs. The lymphatic drainage of FITC-PCE or -SCE into the peritoneal cavity was examined, as previously described (39). Briefly, 100 μg of FITC-labeled PCE or SCE was injected i.p. into mice (two mice per group). After 6 h, mice of each group were killed, and then eight LNs (mesenteric, mediastinal, lumbar, superficial cervical, brachial, axillary, inguinal, and sciatic) were collected in ice-chilled tubes. Single-cell suspensions were prepared from the collected LNs using a cell strainer (BD Biosciences), and then 2.5×10^5 cells were suspended with fluorescence-activated cell sorting (FACS) buffer (PBS containing 0.5% BSA and 2 mM EDTA). The mean fluorescence intensity (MFI) of the samples was measured with an Accuri C6 Plus flow cytometer (BD Biosciences) and analyzed with the FlowJo software (Tree Star).

Analysis of neutrophil recruitment to the peritoneal cavity after injection of different amounts of RN4220-PCE, RN4220-SCE, and USA300-PCE. Mice were injected i.p. with various amounts of RN4220-PCE, RN4220-SCE, or USA300-PCE, as described above. At 12 h postinjection, peritoneal fluids were collected with 5 ml of Hanks balanced salt solution (HBSS) containing 0.5% bovine serum albumin (BSA) and 2 mM EDTA. Peritoneal cells were collected by centrifugation (4°C, $300 \times g$, 5 min) and suspended in 500 μl of MACS buffer (PBS containing 0.5% BSA and 2 mM EDTA). After cell counting by flow cytometry, 1×10^6 cells were suspended in 40 μl of MACS buffer. Five microliters of FcR blocking reagent (130-092-575; Miltenyi Biotech) was added and incubated at 4°C for 10 min. Five microliters of antibody mixture (Ly-6G-APC, F4/80-PE, CD11b-FITC, Ly-6C-PerCP; BD Biosciences) was added and incubated at 4°C for 10 min, and 1 ml of MACS buffer was added. After centrifugation at 4°C and $300 \times g$ for 5 min, pellets were suspended in 200 μl of MACS buffer, and 50,000 cells were analyzed by flow cytometry (Accuri C6 Plus flow cytometer; BD Biosciences). The neutrophil population was calculated using numbers of CD11b$^+$ Ly6G$^+$/F4/80$^-$/Ly-6C^{low} cells by the FlowJo software (Tree Star, Inc.).

Analysis of neutrophils and monocytes in mLNs. Mice were injected i.p. with 40 μg of RN4220-PCE or -SCE, as described above. At 3 h and 6 h postinjection, mLNs were collected, and then a single-cell suspension was prepared using a cell strainer (BD Biosciences). The cells were suspended in FACS buffer. The cell suspension (40 μl) was mixed with 5 μl of FcR blocking reagent and incubated at 4°C for 10 min. To detect neutrophils and monocytes, 10 μl of antibody stock solution was added to each tube, which was then incubated at 4°C for 10 min. Then, 1 ml of FACS buffer was added to each tube for washing, followed by centrifugation at 4°C, $300 \times g$ for 10 min, and then the supernatant was removed. Finally, each pellet was suspended with 100 μl of 4% paraformaldehyde for fixation. After the pellets were washed with FACS buffer, the samples were analyzed using flow cytometry (Accuri C6 Plus flow cytometer; BD) and FlowJo software. Neutrophils and monocytes were identified with Ly-6G$^+$ CD11b$^+$ F4/80$^-$ Ly-6C^{low} and Ly-6G$^-$ CD11b$^+$ F4/80$^+$ Ly-6C^{high} monoclonal antibodies, respectively.

Analyses of dendritic cell population in mLN by flow cytometry. For analyses of the cell populations in mLNs, 40 μg of PCE or SCE was injected i.p. into mice (five per group). At 6 h postinjection, the mLNs were collected and centrifuged at 4°C and $300 \times g$, and the supernatants were removed. Pellets were suspended in 500 μl of FACS buffer. After calculation of the total cell numbers by a flow cytometer, the pellets were suspended in FACS buffer to 5×10^5 cells/40 μl. Flow cytometer analyses were performed as described above. The inflammatory dendritic cells (DCs) were identified by MHC-II$^+$ CD11c$^+$ CD11b$^+$ Ly-6C$^+$ (MHC-II, major histocompatibility complex class II) monoclonal antibody.

Measurement of calprotectin-mediated antibacterial activity. Calprotectin-mediated antibacterial activity was measured by a method reported previously (54). Briefly, after injection of 100 μg of PCE or SCE, 300 μl of collected PFs was incubated with USA300 cells (5×10^6 CFU) in 30% tryptic soy broth (TSB) medium in the presence (0.1 mM) or absence of Paraquat (Sigma-Aldrich). After incubation for 3 h, reaction solutions were spread on tryptic soy agar (TSA) plates. To assess the effects of metal ions, 10 mM MnCl was added to the solution (10 μM final concentration), and then the mixture was incubated at 37°C for 12 h and spread on plates.

Animal experiments. To measure the protective effect of PCE or SCE in a murine model of peritoneal infection, 6-week-old C57BL/6J mice (10 per group) were i.p. injected with SCE or PCE (40 μg). At 12 h postinjection, mice were injected i.p. with 5×10^8 CFU of the *S. aureus* USA300 strain. The mice were observed twice per day for 5 days.

To examine the roles of phagocytes in the PCE-mediated protective effect, 5-week-old C57BL/6J mice (six per group) were injected i.p. with anti-Ly6G MAb (100 μg, clone 1A8; Bio X Cell) or clodronate liposomes (200 μl; FormuMax) (55, 56). As controls, isotype Ab (100 μg, rat IgG2a, clone 2A3; Bio X Cell) and empty liposome (200 μl; FormuMax) were injected.

At 24 h postadministration, peritoneal lavage was carried out with 5 ml of Hanks balanced salt solution (HBSS) containing 0.5% bovine serum albumin (BSA) and 2 mM EDTA. Peritoneal cells were collected by centrifugation (4°C, $300 \times g$, 5 min) and suspended in 500 μl of MACS buffer (PBS containing 0.5% BSA and 2 mM EDTA). After cell counting by flow cytometry, 1×10^6 cells were suspended in 40 μl of MACS buffer. Five microliters of FcR blocking reagent (130-092-575; Miltenyi Biotech) was added and incubated at 4°C for 10 min. Five microliters of antibody mixture (Ly-6G-APC, F4/80-PE, CD11b-FITC, and Ly-6C-PerCP; BD Biosciences) was added and incubated at 4°C for 10 min, and 1 ml of MACS buffer was added. After centrifugation at 4°C and $300 \times g$ for 5 min, pellets were suspended with 100 μl of 4% paraformaldehyde, and 40,000 cells were analyzed by flow cytometry (Accuri C6 flow cytometer Plus; BD). Reduction of the neutrophils and monocytes/macrophages was examined by flow cytometry analysis of peritoneal cavity cells for CD11b$^+$ Ly6G$^+$ (neutrophils), CD11b$^+$ Ly-6G$^-$ (monocytes), F4/80$^+$ CD11b^{high} Ly6C$^-$ (LPMs), and F4/80^{low} CD11b$^+$ Ly6C$^-$ (SPMs). After confirmation of the reduction of neutrophils, monocytes, and macrophages (LPMs and SPMs) by flow cytometry (Fig. S5), the mice ($n = 7$ to 8 mice)

were injected with PCE (40 μg), and 12 h later, they were challenged with i.p. injection of USA300 LAC cells (5×10^8 CFU/mouse). The infected mice were observed for 7 days.

Data processing and statistical analysis. Unless otherwise stated, experiments were carried out at least three times independently, and the results were presented as the mean $\pm$ standard deviation (SD). Other experimental results are representative of at least three independent experiments that yielded similar results. Statistical significance was measured by unpaired Student's *t* test or log rank test with the GraphPad Prism software.

SUPPLEMENTAL MATERIAL

Supplemental material for this article may be found at https://doi.org/10.1128/IAI.00674-19.

SUPPLEMENTAL FILE 1, PDF file, 0.2 MB.
SUPPLEMENTAL FILE 2, PDF file, 0.2 MB.
SUPPLEMENTAL FILE 3, PDF file, 0.1 MB.
SUPPLEMENTAL FILE 4, PDF file, 0.1 MB.
SUPPLEMENTAL FILE 5, PDF file, 0.1 MB.

ACKNOWLEDGMENTS

This research was supported by a PNU-RENovation (2018-2019) project for B.L.L. and by an award from the Indiana University School of Medicine to T.B.

We appreciate Shun-ichiro Kawabata and Toshio Shibata of Kyushu University for helping with the LC-MS analyses.

REFERENCES

1. Tong SY, Davis JS, Eichenberger E, Holland TL, Fowler VG, Jr. 2015. Staphylococcus aureus infections: epidemiology, pathophysiology, clinical manifestations, and management. Clin Microbiol Rev 28:603–661. https://doi.org/10.1128/CMR.00134-14.
2. Missiakas D, Schneewind O. 2016. Staphylococcus aureus vaccines: deviating from the carol. J Exp Med 213:1645–1653. https://doi.org/10.1084/jem.20160569.
3. Proctor RA. 2012. Challenges for a universal Staphylococcus aureus vaccine. Clin Infect Dis 54:1179–1186. https://doi.org/10.1093/cid/cis033.
4. Iwasaki A, Medzhitov R. 2010. Regulation of adaptive immunity by the innate immune system. Science 327:291–295. https://doi.org/10.1126/science.1183021.
5. Schmaler M, Jann NJ, Gotz F, Landmann R. 2010. Staphylococcal lipoproteins and their role in bacterial survival in mice. Int J Med Microbiol 300:155–160. https://doi.org/10.1016/j.ijmm.2009.08.018.
6. Weidenmaier C, Peschel A. 2008. Teichoic acids and related cell-wall glycopolymers in Gram-positive physiology and host interactions. Nat Rev Microbiol 6:276–287. https://doi.org/10.1038/nrmicro1861.
7. Kurokawa K, Takahashi K, Lee BL. 2016. The staphylococcal surface-glycopolymer wall teichoic acid (WTA) is crucial for complement activation and immunological defense against Staphylococcus aureus infection. Immunobiology 221:1091–1101. https://doi.org/10.1016/j.imbio.2016.06.003.
8. Zeng Z, Surewaard BG, Wong CH, Geoghegan JA, Jenne CN, Kubes P. 2016. CRIg functions as a macrophage pattern recognition receptor to directly bind and capture blood-borne Gram-positive bacteria. Cell Host Microbe 20:99–106. https://doi.org/10.1016/j.chom.2016.06.002.
9. Fournier B, Philpott DJ. 2005. Recognition of Staphylococcus aureus by the innate immune system. Clin Microbiol Rev 18:521–540. https://doi.org/10.1128/CMR.18.3.521-540.2005.
10. Strominger JL. 1965. Biochemistry of the cell wall of Staphylococcus aureus. Ann N Y Acad Sci 128:59–61. https://doi.org/10.1111/j.1749-6632.1965.tb11629.x.
11. Park JW, Kim CH, Kim JH, Je BR, Roh KB, Kim SJ, Lee HH, Ryu JH, Lim JH, Oh BH, Lee WJ, Ha NC, Lee BL. 2007. Clustering of peptidoglycan recognition protein-SA is required for sensing lysine-type peptidoglycan in insects. Proc Natl Acad Sci U S A 104:6602–6607. https://doi.org/10.1073/pnas.0610924104.
12. Foster TJ, Geoghegan JA, Ganesh VK, Hook M. 2014. Adhesion, invasion and evasion: the many functions of the surface proteins of Staphylococcus aureus. Nat Rev Microbiol 12:49–62. https://doi.org/10.1038/nrmicro3161.
13. Gerlach D, Guo Y, De Castro C, Kim SH, Schlatterer K, Xu FF, Pereira C, Seeberger PH, Ali S, Codee J, Sirisarn W, Schulte B, Wolz C, Larsen J, Molinaro A, Lee BL, Xia G, Stehle T, Peschel A. 2018. Methicillin-resistant Staphylococcus aureus alters cell wall glycosylation to evade immunity. Nature 563:705–709. https://doi.org/10.1038/s41586-018-0730-x.
14. Storni T, Kundig TM, Senti G, Johansen P. 2005. Immunity in response to particulate antigen-delivery systems. Adv Drug Deliv Rev 57:333–355. https://doi.org/10.1016/j.addr.2004.09.008.
15. Kool M, Fierens K, Lambrecht BN. 2012. Alum adjuvant: some of the tricks of the oldest adjuvant. J Med Microbiol 61:927–934. https://doi.org/10.1099/jmm.0.038943-0.
16. Kuroda E, Coban C, Ishii KJ. 2013. Particulate adjuvant and innate immunity: past achievements, present findings, and future prospects. Int Rev Immunol 32:209–220. https://doi.org/10.3109/08830185.2013.773326.
17. Kurokawa K, Jung DJ, An JH, Fuchs K, Jeon YJ, Kim NH, Li X, Tateishi K, Park JA, Xia G, Matsushita M, Takahashi K, Park HJ, Peschel A, Lee BL. 2013. Glycoepitopes of staphylococcal wall teichoic acid govern complement-mediated opsonophagocytosis via human serum antibody and mannose-binding lectin. J Biol Chem 288:30956–30968. https://doi.org/10.1074/jbc.M113.509893.
18. Lee JH, Kim NH, Winstel V, Kurokawa K, Larsen J, An JH, Khan A, Seong MY, Lee MJ, Andersen PS, Peschel A, Lee BL. 2015. Surface glycopolymers are crucial for in vitro anti-wall teichoic acid IgG-mediated complement activation and opsonophagocytosis of Staphylococcus aureus. Infect Immun 83:4247–4255. https://doi.org/10.1128/IAI.00767-15.
19. Xia G, Maier L, Sanchez-Carballo P, Li M, Otto M, Holst O, Peschel A. 2010. Glycosylation of wall teichoic acid in Staphylococcus aureus by TarM. J Biol Chem 285:13405–13415. https://doi.org/10.1074/jbc.M109.096172.
20. Tokunaga M, Tokunaga H, Wu HC. 1982. Post-translational modification and processing of Escherichia coli prolipoprotein in vitro. Proc Natl Acad Sci U S A 79:2255–2259. https://doi.org/10.1073/pnas.79.7.2255.
21. Nair D, Memmi G, Hernandez D, Bard J, Beaume M, Gill S, Francois P, Cheung AL. 2011. Whole-genome sequencing of Staphylococcus aureus strain RN4220, a key laboratory strain used in virulence research, identifies mutations that affect not only virulence factors but also the fitness of the strain. J Bacteriol 193:2332–2335. https://doi.org/10.1128/JB.00027-11.
22. Rom JS, Atwood DN, Beenken KE, Meeker DG, Loughran AJ, Spencer HJ, Lantz TL, Smeltzer MS. 2017. Impact of Staphylococcus aureus regulatory mutations that modulate biofilm formation in the USA300 strain LAC on virulence in a murine bacteremia model. Virulence 8:1776–1790. https://doi.org/10.1080/21505594.2017.1373926.
23. Ghosn EE, Cassado AA, Govoni GR, Fukuhara T, Yang Y, Monack DM, Bortoluci KR, Almeida SR, Herzenberg LA, Herzenberg LA. 2010. Two physically, functionally, and developmentally distinct peritoneal macro-

phage subsets. Proc Natl Acad Sci U S A 107:2568–2573. https://doi.org/10.1073/pnas.0915000107.
24. Sethi S, Chakraborty T. 2011. Role of TLR-/NLR-signaling and the associated cytokines involved in recruitment of neutrophils in murine models of Staphylococcus aureus infection. Virulence 2:316–328. https://doi.org/10.4161/viru.2.4.16142.
25. Teigelkamp S, Bhardwaj RS, Roth J, Meinardus-Hager G, Karas M, Sorg C. 1991. Calcium-dependent complex assembly of the myeloic differentiation proteins MRP-8 and MRP-14. J Biol Chem 266:13462–13467.
26. Corbin BD, Seeley EH, Raab A, Feldmann J, Miller MR, Torres VJ, Anderson KL, Dattilo BM, Dunman PM, Gerads R, Caprioli RM, Nacken W, Chazin WJ, Skaar EP. 2008. Metal chelation and inhibition of bacterial growth in tissue abscesses. Science 319:962–965. https://doi.org/10.1126/science.1152449.
27. Urban CF, Ermert D, Schmid M, Abu-Abed U, Goosmann C, Nacken W, Brinkmann V, Jungblut PR, Zychlinsky A. 2009. Neutrophil extracellular traps contain calprotectin, a cytosolic protein complex involved in host defense against Candida albicans. PLoS Pathog 5:e1000639. https://doi.org/10.1371/journal.ppat.1000639.
28. Zackular JP, Chazin WJ, Skaar EP. 2015. Nutritional immunity: S100 proteins at the host-pathogen interface. J Biol Chem 290:18991–18998. https://doi.org/10.1074/jbc.R115.645085.
29. Lopes AT, Manso C. 1989. Paraquat and diquat: mechanisms of toxicity. Acta Med Port 2:35–39. (In Portuguese.)
30. Abbitt KB, Cotter MJ, Ridger VC, Crossman DC, Hellewell PG, Norman KE. 2009. Antibody ligation of murine Ly-6G induces neutropenia, blood flow cessation, and death via complement-dependent and independent mechanisms. J Leukoc Biol 85:55–63. https://doi.org/10.1189/jlb.0507305.
31. van Rooijen N, Sanders A, van den Berg TK. 1996. Apoptosis of macrophages induced by liposome-mediated intracellular delivery of clodronate and propamidine. J Immunol Methods 193:93–99. https://doi.org/10.1016/0022-1759(96)00056-7.
32. Sunderkötter C, Nikolic T, Dillon MJ, Van Rooijen N, Stehling M, Drevets DA, Leenen PJ. 2004. Subpopulations of mouse blood monocytes differ in maturation stage and inflammatory response. J Immunol 172:4410–4417. https://doi.org/10.4049/jimmunol.172.7.4410.
33. Kieser KJ, Kagan JC. 2017. Multi-receptor detection of individual bacterial products by the innate immune system. Nat Rev Immunol 17:376–390. https://doi.org/10.1038/nri.2017.25.
34. Goodridge HS, Reyes CN, Becker CA, Katsumoto TR, Ma J, Wolf AJ, Bose N, Chan AS, Magee AS, Danielson ME, Weiss A, Vasilakos JP, Underhill DM. 2011. Activation of the innate immune receptor dectin-1 upon formation of a 'phagocytic synapse'. Nature 472:471–475. https://doi.org/10.1038/nature10071.
35. Sharp FA, Ruane D, Claass B, Creagh E, Harris J, Malyala P, Singh M, O'Hagan DT, Pétrilli V, Tschopp J, O'Neill LAJ, Lavelle EC. 2009. Uptake of particulate vaccine adjuvants by dendritic cells activates the NALP3 inflammasome. Proc Natl Acad Sci U S A 106:870–875. https://doi.org/10.1073/pnas.0804897106.
36. Hornung V, Bauernfeind F, Halle A, Samstad EO, Kono H, Rock KL, Fitzgerald KA, Latz E. 2008. Silica crystals and aluminum salts activate the NALP3 inflammasome through phagosomal destabilization. Nat Immunol 9:847–856. https://doi.org/10.1038/ni.1631.
37. Muruve DA, Petrilli V, Zaiss AK, White LR, Clark SA, Ross PJ, Parks RJ, Tschopp J. 2008. The inflammasome recognizes cytosolic microbial and host DNA and triggers an innate immune response. Nature 452:103–107. https://doi.org/10.1038/nature06664.
38. Vanlangenakker N, Vanden Berghe T, Krysko DV, Festjens N, Vandenabeele P. 2008. Molecular mechanisms and pathophysiology of necrotic cell death. Curr Mol Med 8:207–220. https://doi.org/10.2174/156652408784221306.
39. Marco AJ, Domingo M, Ruberte J, Carretero A, Briones V, Dominguez L. 1992. Lymphatic drainage of Listeria monocytogenes and Indian ink inoculated in the peritoneal cavity of the mouse. Lab Anim 26:200–205. https://doi.org/10.1258/002367792780740549.
40. Lim SY, Raftery M, Cai H, Hsu K, Yan WX, Hseih HL, Watts RN, Richardson D, Thomas S, Perry M, Geczy CL. 2008. S-nitrosylated S100A8: novel anti-inflammatory properties. J Immunol 181:5627–5636. https://doi.org/10.4049/jimmunol.181.8.5627.
41. McGuinness WA, Kobayashi SD, DeLeo FR. 2016. Evasion of neutrophil killing by Staphylococcus aureus. Pathogens 5:32. https://doi.org/10.3390/pathogens5010032.
42. Otto M. 2014. Staphylococcus aureus toxins. Curr Opin Microbiol 17:32–37. https://doi.org/10.1016/j.mib.2013.11.004.
43. Spaan AN, van Strijp JAG, Torres VJ. 2017. Leukocidins: staphylococcal bi-component pore-forming toxins find their receptors. Nat Rev Microbiol 15:435–447. https://doi.org/10.1038/nrmicro.2017.27.
44. Novick RP, Ross HF, Projan SJ, Kornblum J, Kreiswirth B, Moghazeh S. 1993. Synthesis of staphylococcal virulence factors is controlled by a regulatory RNA molecule. EMBO J 12:3967–3975. https://doi.org/10.1002/j.1460-2075.1993.tb06074.x.
45. Oku Y, Kurokawa K, Matsuo M, Yamada S, Lee BL, Sekimizu K. 2009. Pleiotropic roles of polyglycerolphosphate synthase of lipoteichoic acid in growth of Staphylococcus aureus cells. J Bacteriol 191:141–151. https://doi.org/10.1128/JB.01221-08.
46. Kurokawa K, Lee H, Roh KB, Asanuma M, Kim YS, Nakayama H, Shiratsuchi A, Choi Y, Takeuchi O, Kang HJ, Dohmae N, Nakanishi Y, Akira S, Sekimizu K, Lee BL. 2009. The triacylated ATP binding cluster transporter substrate-binding lipoprotein of Staphylococcus aureus functions as a native ligand for Toll-like receptor 2. J Biol Chem 284:8406–8411. https://doi.org/10.1074/jbc.M809618200.
47. Brown S, Xia G, Luhachack LG, Campbell J, Meredith TC, Chen C, Winstel V, Gekeler C, Irazoqui JE, Peschel A, Walker S. 2012. Methicillin resistance in Staphylococcus aureus requires glycosylated wall teichoic acids. Proc Natl Acad Sci U S A 109:18909–18914. https://doi.org/10.1073/pnas.1209126109.
48. Moore BW. 1965. A soluble protein characteristic of the nervous system. Biochem Biophys Res Commun 19:739–744. https://doi.org/10.1016/0006-291X(65)90320-7.
49. Shiratsuchi A, Shimizu K, Watanabe I, Hashimoto Y, Kurokawa K, Razanajatovo IM, Park KH, Park HK, Lee BL, Sekimizu K, Nakanishi Y. 2010. Auxiliary role for D-alanylated wall teichoic acid in Toll-like receptor 2-mediated survival of Staphylococcus aureus in macrophages. Immunology 129:268–277. https://doi.org/10.1111/j.1365-2567.2009.03168.x.
50. Enghofer E, Kress H. 1979. An evaluation of the Morgan-Elson assay for 2-amino-2-deoxy sugars. Carbohydr Res 76:233–238. https://doi.org/10.1016/0008-6215(79)80022-1.
51. Leong MM, Milstein C, Pannell R. 1986. Luminescent detection method for immunodot, Western, and Southern blots. J Histochem Cytochem 34:1645–1650. https://doi.org/10.1177/34.12.3537113.
52. Tino MJ, Wright JR. 1996. Surfactant protein A stimulates phagocytosis of specific pulmonary pathogens by alveolar macrophages. Am J Physiol 270:L677–L688. https://doi.org/10.1152/ajplung.1996.270.4.L677.
53. Geertsma MF, Nibbering PH, Haagsman HP, Daha MR, van Furth R. 1994. Binding of surfactant protein A to C1q receptors mediates phagocytosis of Staphylococcus aureus by monocytes. Am J Physiol 267:L578–L584. https://doi.org/10.1152/ajplung.1994.267.5.L578.
54. Kehl-Fie TE, Chitayat S, Hood MI, Damo S, Restrepo N, Garcia C, Munro KA, Chazin WJ, Skaar EP. 2011. Nutrient metal sequestration by calprotectin inhibits bacterial superoxide defense, enhancing neutrophil killing of Staphylococcus aureus. Cell Host Microbe 10:158–164. https://doi.org/10.1016/j.chom.2011.07.004.
55. Park SJ, Wiekowski MT, Lira SA, Mehrad B. 2006. Neutrophils regulate airway responses in a model of fungal allergic airways disease. J Immunol 176:2538–2545. https://doi.org/10.4049/jimmunol.176.4.2538.
56. Hurt M, Neelam S, Niederkorn J, Alizadeh H. 2003. Pathogenic Acanthamoeba spp. secrete a mannose-induced cytolytic protein that correlates with the ability to cause disease. Infect Immun 71:6243–6255. https://doi.org/10.1128/iai.71.11.6243-6255.2003.